Effusive intermediate glaciovolcanism in the Garibaldi Volcanic Belt, southwestern British Columbia, Canada

M. C. KELMAN[1], J. K. RUSSELL[1] & C. J. HICKSON[2]

[1] *Igneous Petrology Laboratory, Department of Earth and Ocean Sciences, University of British Columbia, 6339 Stores Road, Vancouver, British Columbia V6T 1Z4, Canada (e-mail: mkelman@eos.ubc.ca)*

[2] *Geological Survey of Canada, 101-605 Robson Street, Vancouver, British Columbia V6B 5J3, Canada*

Abstract: The Garibaldi Volcanic Belt (GVB) in southwestern British Columbia is dominated by intermediate composition volcanoes in a setting that has been intermittently subjected to widespread glaciation. The glaciovolcanic features produced are distinctive, and include flow-dominated tuyas, subglacial domes, and ice-marginal flows. Flow-dominated tuyas, which are intermediate in composition, are unlike conventional basaltic tuyas; they consist of stacks of flat-lying lava flows, and lack pillows and hyaloclastite. They are inferred to represent subglacial eruptions that ultimately breached the ice surface. Subglacial domes occur as steep-sided masses of heavily-jointed, glassy lava, and represent eruptions that were entirely subglacial. Ice-marginal flows derive from subaerial flows that were impounded against ice.

Two unique aspects of GVB glaciovolcanic products are the presence of flow-dominated tuyas and the apparent scarcity of primary fragmental deposits. These unique features result from lava composition, the minimization of direct lava–water contact during eruptions, and topography. Composition influences morphology because eruption temperature decreases, and viscosity and glass transition temperature both increase with silica content. The result of this is that silicic subglacial volcanoes melt less water and are less likely to trap it near the vent, leading to the formation of structures whose shapes are strongly influenced by the surrounding ice. Topography also enhances meltwater drainage, favours lava flow impoundment in ice-filled valleys, and may, through erosion, influence the observed distribution of fragmental glaciovolcanic deposits.

Southwestern British Columbia is a region of extensive Neogene–Quaternary volcanism, and the waxing and waning of continental-scale ice sheets, as well as the presence of alpine glaciers, during Quaternary time has led to many interactions between volcanoes and ice. These interactions explain numerous geomorphological features of southwestern British Columbia's Garibaldi Volcanic Belt (GVB).

In this paper, we aim to (1) introduce the GVB and its glaciovolcanic landforms, (2) highlight the unique aspects of GVB glaciovolcanic deposits, and (3) discuss the origins of some of the more distinctive glaciovolcanic landforms in the GVB. Glaciovolcanic features of the GVB are substantially different from those described in Iceland (Jones 1966, 1969, 1970; Furnes *et al.* 1980; Tuffen *et al.* 2001), Antarctica (Smellie *et al.* 1993; Smellie & Skilling 1994; Smellie 2000), and other parts of British Columbia (Mathews 1947; Souther 1992; Hickson 1987; Hickson *et al.* 1995; Edwards & Russell 2002; Edwards *et al.* 2002). The three main landforms resulting from intermediate composition glaciovolcanism are: flow-dominated tuyas, subglacial domes and ice-marginal lava flows. Pillows and fragmental material are rare or absent at all three types of landform. The unique aspects of GVB glaciovolcanic landforms reflect lava compositions and terrain.

The landforms and lithologic features formed by glaciovolcanism are distinctive. Where these deposits are preserved, they can serve as an important palaeoclimatological tool, because they provide an indicator of the past presence of ice. Additionally, an understanding of how volcanoes and ice interact is important for hazard assessments, since subglacial eruptions have the potential to release catastrophically large volumes of water (as jökulhlaups) due to

From: SMELLIE, J. L. & CHAPMAN, M. G. (eds) 2002. *Volcano–Ice Interaction on Earth and Mars*. Geological Society, London, Special Publications, **202**, 195–211. 0305-8719/02/$15.00

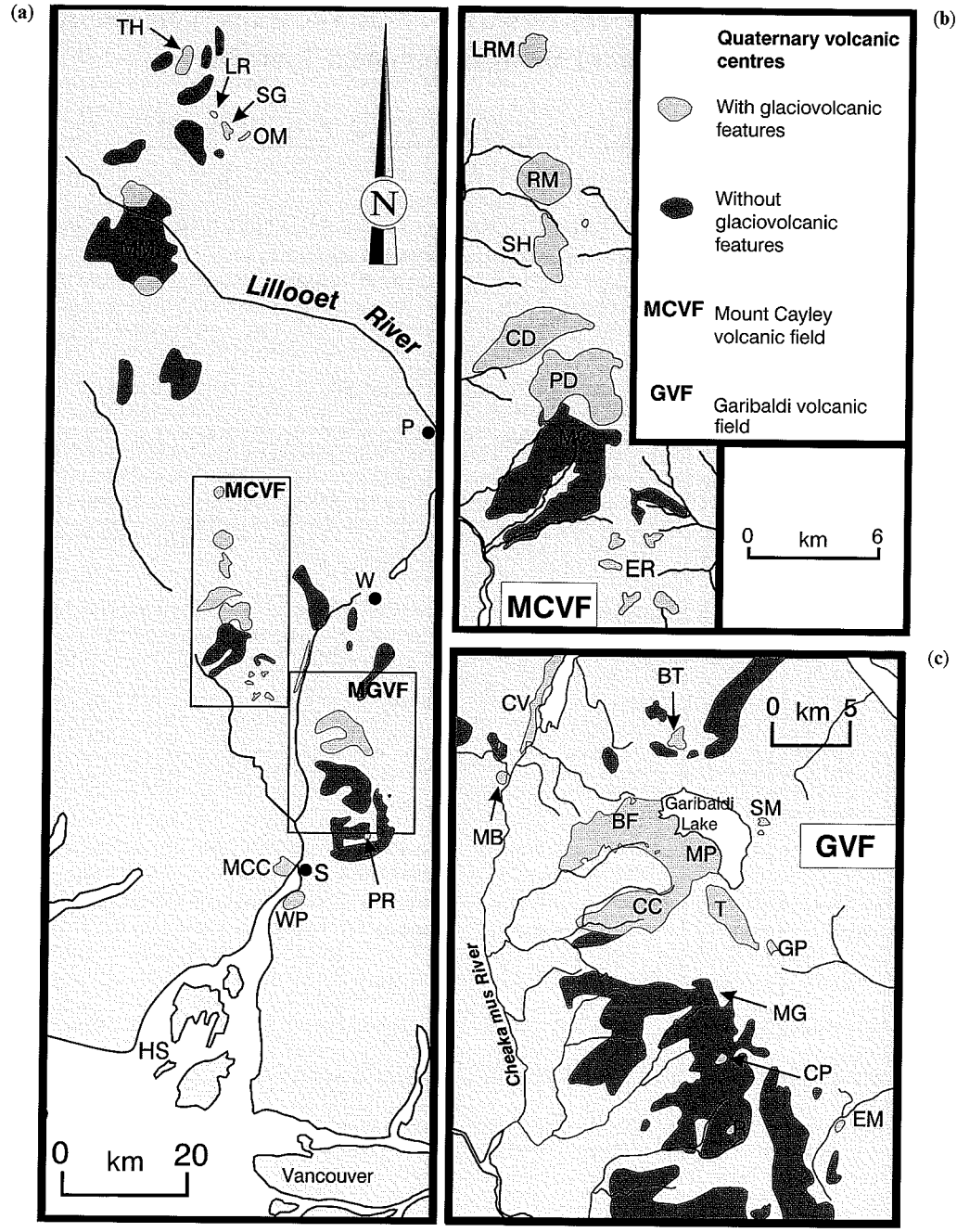

Fig. 1. (**a**) Map of the Garibaldi Volcanic Belt, showing the distribution of volcanic centres (after Hickson 1994). (**b**) Map of the Mount Cayley volcanic field (after Souther 1980). (**c**) Map of the Garibaldi volcanic field. Individual glaciovolcanic centres are abbreviated as follows: BF, Barrier flow; BT, Black Tusk; CC, Culliton Creek flow; CD, Cauldron Dome; CP, Columnar Peak; CV, Cheakamus Valley flows; EM, Eenostuck mass; ER, Ember Ridge; GP, Glacier Pikes; HS, Howe Sound; LR, Logan Ridge; LRM, Little Ring Mountain; MB, Mount Brew; MCC, Monmouth Creek complex; MC, Mount Cayley; MG, Mount Garibaldi; MM, Mount Meager; MP, Mount Price; OM, Ochre Mountain; P, Pemberton; PD, Pali Dome; PR, Paul Ridge; R, Round Mountain; RM, Ring Mountain; S, Squamish; SG, Salal Glacier volcanic complex; SH, Slag Hill; SM, Sphinx Moraine; T, Table; TH, Tuber Hill; W, Whistler; WP, Watts Point. Silverthrone Mountain, at the northern extent of the Garibaldi Volcanic Belt, lies to the north of the area covered by this map.

rapid, large-scale melting of ice. Finally, distributions of products of glaciovolcanism can be used to constrain temporal and spatial linkages between volcanism and glaciation.

Garibaldi Volcanic Belt

The Garibaldi Volcanic Belt (Fig. 1) of southwestern British Columbia is the northern extension of the Cascade magmatic arc of the western United States (Green *et al.* 1988; Guffanti & Weaver 1988; Read 1990; Sherrod & Smith 1990; Hickson 1994). It extends from Mount Garibaldi, which is located near the head of Howe Sound, northward through the Salal Glacier volcanic complex to Silverthrone Mountain. Volcanic deposits in the GVB range from Miocene to Holocene in age, and are principally a result of the subduction of the Juan de Fuca plate beneath the North American plate (Green *et al.* 1988; Rohr *et al.* 1996). There are at least eight separate volcanic complexes in the GVB (Table 1), which include stratovolcanoes, isolated flows, domes, spines, cones and tuyas ranging in composition from high-alumina basalt to rhyolite (Fig. 2). The most recent eruption occurred at Mount Meager at 2360 BP (Clague *et al.* 1995; Leonard 1995).

Glaciovolcanic features have been recognized at Watts Point (Bye *et al.* 2000), the Monmouth Creek complex, Garibaldi volcanic field, (Mathews 1951, 1952*a*,*b*, 1958; Green 1977), the Mount Cayley volcanic field (Souther 1980; Kelman *et al.* 2001), Mount Meager and the Salal Glacier region (Lawrence *et al.* 1984; Roddick & Souther 1987; Green *et al.* 1988; Fig. 1). The sizes, ages and lithologic attributes of these landforms are summarized in Table 2.

Isotopic studies on deep-sea sediments show that there have been eight major climatic cycles in southern British Columbia over the past 800 000 years (Shackleton & Opdyke 1973). Many of these cycles were accompanied by widespread, though not necessarily continental-scale, glaciations (Clague *et al.* 1982); ice may have been confined to regions between mountain ranges (Clague 1986). There have been at least two major glaciations in the Canadian Cordillera during the past 100 000 years (Fulton 1984). The Fraser Glaciation, in southwestern British Columbia, began at about 25 000–30 000 BP, peaked at about 14 000–14 500 BP, and was in retreat by about 10 000 BP (Fulton 1971; Clague 1980, 1981). The timing of earlier glaciations is poorly known, but stratigraphic evidence for pre-Wisconsinan ice sheets in the western Canadian Cordillera does exist (e.g. Denton & Stuiver 1967; Klassen 1978; Armstrong 1981). Past glacial episodes and their timing with respect to glaciovolcanic events in the GVB are shown in Figure 3. Further dating of glaciovolcanic deposits within southwestern British Columbia would elucidate Quaternary glaciochronologies.

Glaciovolcanic landforms

Tuyas

Within the GVB, there are a number of tuya-shaped edifices which lack the internal stratigraphy described for basaltic tuyas (Mathews 1947; Jones 1966, 1969). These volcanic landforms, herein termed flow-dominated tuyas, comprise masses of intensely jointed, intermediate composition lava flows that have flat tops and steep sides, and have few or no pillow lavas or

Table 1. *Quaternary volcanic centres of the Garibaldi Volcanic Belt*

Major centres and fields	Composition*	Age	Source†
Silverthrone volcanic field	BA to R	1 to 0.4 Ma	1
Franklin Glacier complex	D, A	3.9 to 2.2 Ma	1
Salal Glacier volcanic field	AOB, H	1 to 0.6 Ma	2
Mount Meager–Elaho Valley	B to D	2.2 Ma to 2.4 ka	3, 4, 5
Mount Cayley volcanic field	BA to RD	0.5 to 0.3 Ma	3
Garibaldi volcanic field	B to D	1.3 Ma to 10 ka	3, 6, 7
Monmouth Creek complex	BA to D	nd‡	8
Watts Point volcanic field	D	130 to 90 ka	3

* AOB, alkali olivine basalt; H, hawaiite; B, basalt; BA, basaltic andesite; A, andesite; D = dacite; RD, rhyodacite; R, rhyolite.

† 1, Souther & Yorath 1991; 2, Lawrence *et al.* 1984; 3, Green *et al.* 1988; 4, Leonard 1995; 5, Clague *et al.* 1995; 6, Mathews 1958; 7, Brooks & Friele 1992; 8, Green 1994.

‡ nd, not determined.

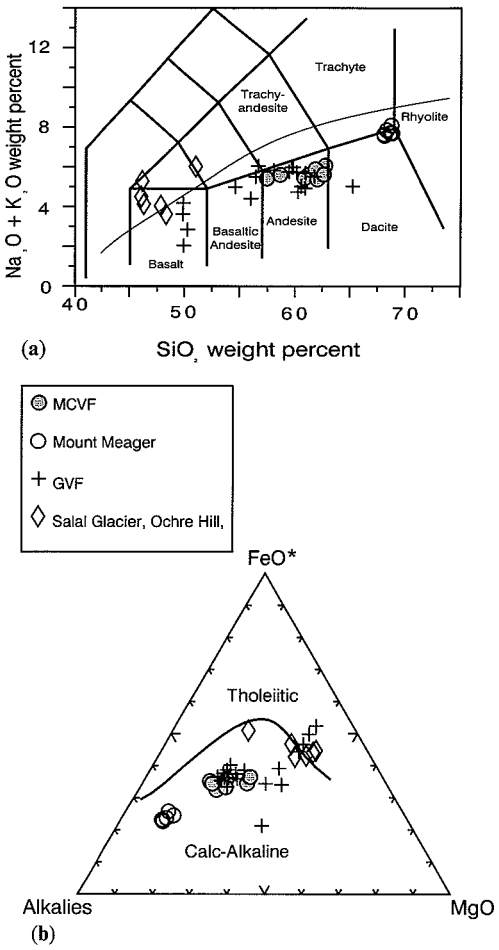

Fig. 2. Chemical classification of volcanic rocks from the Garibaldi Volcanic Belt. Data are for the Mount Cayley volcanic field (Kelman *et al.* 2001), Mount Meager (Stasiuk & Russell 1990; Hickson *et al.* 1999), Garibaldi volcanic field (Mathews 1957; Green 1977), and Salal Glacier volcanic field, Ochre Hill and Logan Ridge (Lawrence *et al.* 1984). Abbreviations used are the same as in Figure 1. (**a**) Total alkalis v. silica. Fields are from LeBas *et al.* (1986). The curved line is the alkaline–subalkaline division of Irvine & Baragar (1971). (**b**) AFM diagram (Irvine & Baragar 1971), showing the dominance of calc-alkaline compositions in the Garibaldi Volcanic Belt.

fragmental deposits. The Table (Fig. 4a), located to the north of Mount Garibaldi (Fig. 1), exemplifies this type of landform. It consists of a nearly vertical-sided stack of flat-lying hornblende-phyric andesite lava sheets, partially coated by thin, nearly vertical, lava sheets. Horizontal or nearly horizontal columns occur at numerous locations along the periphery of the mass.

Two other flow-dominated tuyas occur in the northern Mount Cayley volcanic field (Fig. 1). Ring Mountain is a nearly circular feature of unknown age, composed of a sequence of flows of glassy, plagioclase–orthopyroxene–phyric andesite. The uppermost, horizontal flows are coarsely jointed and separated by layers of oxidized scoria. On Ring Mountain's western side, outcrops contain highly variable, fine-scale jointing and are locally broken down into many small spires and knobs. Little Ring Mountain (Fig. 4b, c) is smaller but otherwise similar in morphology and jointing characteristics to Ring Mountain, and may be of similar age. Its eruptive products are fine-grained to glassy black plagioclase-augite-phyric andesite flows (Kelman *et al.* 2001).

Cauldron Dome, in the central Mount Cayley volcanic field (Fig. 1), has a complex structure. It has an elliptical shape in plan view, and comprises a flat-topped stack of hypersthene-phyric andesite flows. Lower flows are coarsely jointed and commonly oxidized; their margins form vertical cliffs. The upper Cauldron Dome flows have more intense, variable, and fine-scale jointing than the lower flows, are commonly glassy, and form near-vertical cliffs featuring many small spires and knobs.

The shapes and joint characteristics of flow-dominated tuyas cannot be explained by the apparent palaeotopography. For example, these steep sided masses were clearly not the result of lava filling palaeovalleys. Thus, they are inferred to have originated from subglacial eruptions.

The top surfaces of the Table, Ring Mountain, and Little Ring Mountain represent subaerial emplacement, and these edifices are likely monogenetic. Cauldron Dome, however, probably results from multiple eruptions. Its lower flows appear to be subaerial; these flows form precipitous cliffs whose steepness is a result of erosion, and there is no evidence for quenching by ice. The upper Cauldron Dome flows appear to have formed subglacially, although it is unclear whether the uppermost surface of Cauldron Dome represents subglacial or subaerial eruption.

Flow-dominated tuyas, thus, are characterized by (a) stacked, relatively flat-lying lava flows; (b) upper surfaces which are subaerial in origin; (c) horizontal columns at the lateral margins, indicating vertical cooling surfaces; (d) irregular, fine-scale, columnar jointing at the lateral margins, indicating rapid cooling; and (e) edifice shapes and joint patterns which cannot be explained by known palaeotopography. These features are consistent with subglacial eruptions that ultimately breached the ice surface.

Table 2. *Summary and description of glaciovolcanic features in the Garibaldi Volcanic Belt*

Name	Feature*	Rock type†	Area (m)	Height (m)	Age/Glacial period	Source‡
Tuber Hill	T	B	2000 × 2000	<450	0.598 ± 0.015; 0.731 ± 0.037; 0.760 ± 0.033	1
Little Ring Mountain	T	A	120 × 120	270	?	2
Ring Mountain	T	A	200 × 200	590	?	2
Slag Hill	SGD, T	A, BA	1540 × 3000	<700	?	3
Cauldron Dome	T	A	4100 × 2100	<400	0.49 ± 0.08	3, 4
Ember Ridge (6 domes)	SGD	A	180 × 260 to 1060 × 1080	<300	?	3
Cheakamus Valley flows	SGF	B	<1600 × 50–100	10–20	Fraser Glaciation	5, 6
Mount Brew	SGD	A	?	?	?	4
Sphinx Moraine complex	SGD	BA	?	>30	pre-Fraser Glaciation	6
Table	T	A	300 × 180	250	Fraser Glaciation	7
Columnar Peak	SGD	D	?	?	?	4, 8
Eenostuck Mass	SGD	BA	800 × 180	90	Fraser Glaciation?	8
Monmouth Creek complex	?	D, BA	1000? × 600?	~150	?	8
Watts Point	SGD	D	700 × 600	< 100	0.09 ± 0.03; 0.13 ± 0.03	4, 9

* T, tuya; SGD, subglacial dome; SGF, subglacial flow.
† B, basalt; BA, basaltic andesite; A, andesite; D, dacite.
‡ 1, Roddick & Souther 1987; 2, Kelman *et al.* 2001; 3, Souther 1980; 4, Green *et al.* 1988; 5, Mathews 1952*b*: 6, Green 1977; 7, Mathews 1951; 8, Mathews 1958; 9, Bye *et al.* 2000.

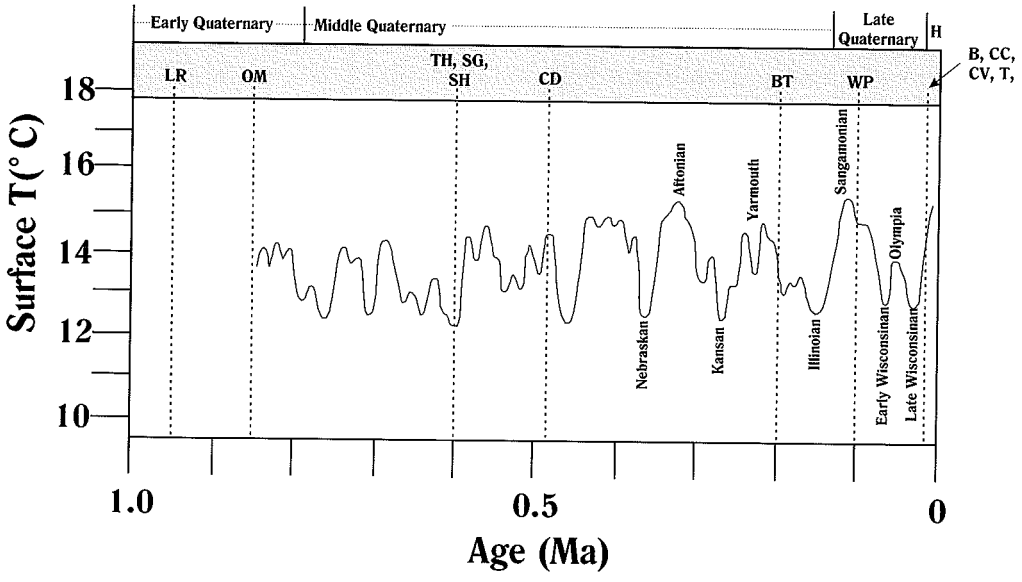

Fig. 3. Timing of Garibaldi Volcanic Belt glaciations and glaciovolcanic events during the last 1 million years. Curve shows surface temperature variations during the last 850 000 years (Gribbin 1990). Peaks represent interglacial intervals whereas troughs represent glacial intervals. Dashed vertical lines show glaciovolcanic events in the Garibaldi Volcanic Belt whose ages are known (Table 2), using the abbreviations in Figure 1. Uncertainties in K–Ar dates are variable and are as great as 0.1 Ma for some dates, but are not shown for simplicity. Some events for which there are no radiometric dates available are placed in the Late Wisconsinan because they contain glaciovolcanic features with no evidence of subsequent glacial overriding. H, Holocene.

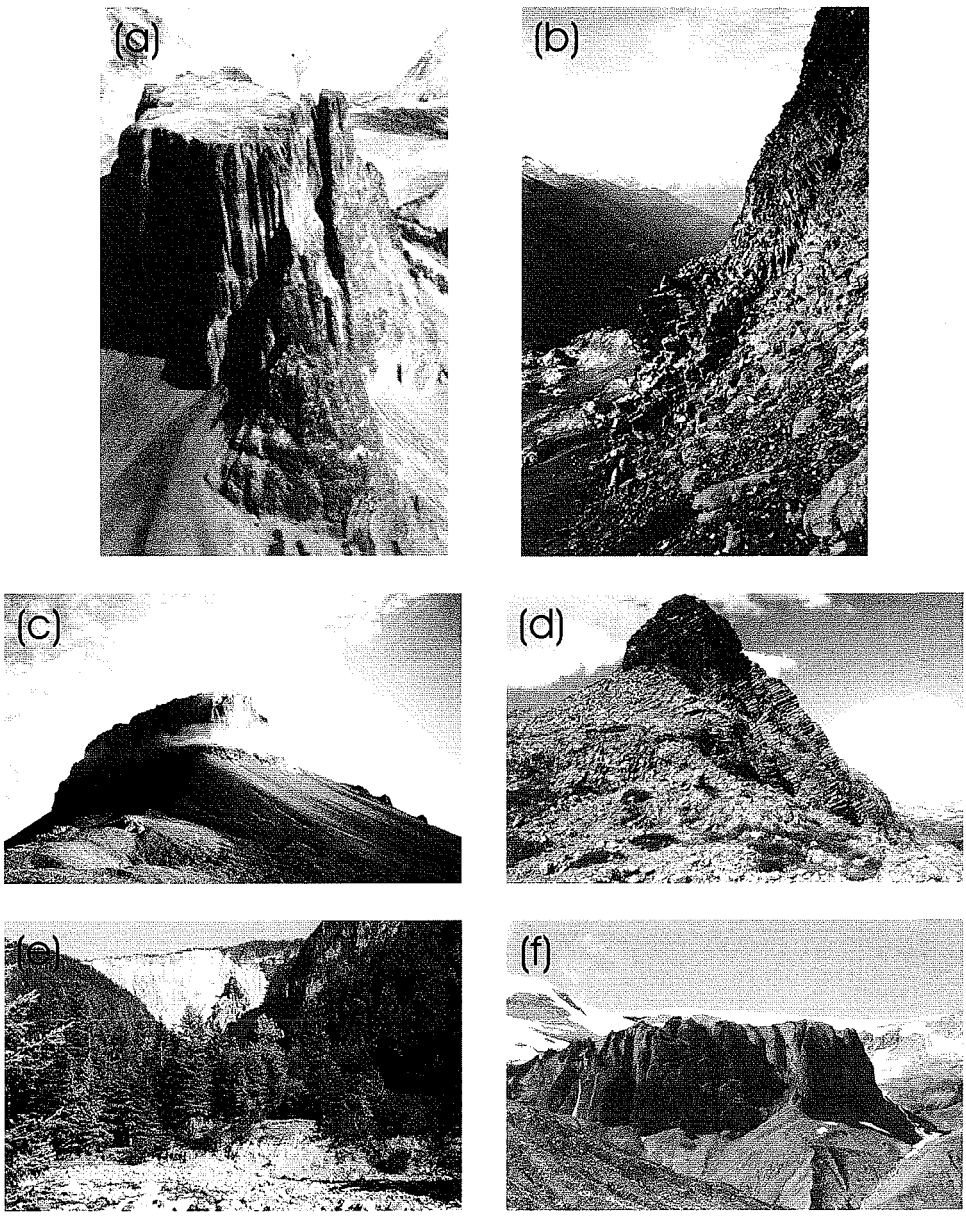

Fig. 4. Glaciovolcanic features in the Garibaldi Volcanic Belt. (**a**) The Table, a flow-dominated tuya in the Garibaldi volcanic field. Its height is approximately 260 m. (**b**) Columnar joints on the east side of Little Ring Mountain. Columns at the top are subvertical, whereas columns near the bottom are nearly horizontal. Columns near the bottom are approximately are 30–50 cm across. Scale is also indicated by the climber at the lower left of the image. (**c**) Little Ring Mountain, a flow-dominated tuya in the northern Mount Cayley volcanic field. Its height is approximately 250 m. (**d**) One of the six subglacial domes of the Ember Ridge deposit in the Mount Cayley volcanic field. Height of the visible outcrop is approximately 30 m. (**e**) The Barrier, an ice-marginal flow in the Garibaldi volcanic field, which truncates abruptly in a 200 m cliff overlooking the valley floor. The photograph is taken standing down-valley, on deposits from a major landslide from the Barrier during the mid-nineteenth century. (**f**) Ice-contact cliffs at the eastern margin of Pali Dome, approximately 100 m high. Material at the top of the cliffs, and the debris below, is glassy. Jointing along the cliff tops is fine-scale, and column orientations are locally variable.

Subglacial domes

Subglacial domes are another prominent morphological feature common to the GVB, consisting of steep-sided, dome-shaped lava flows with fine-scale jointing. Pillows and fragmental material, such as hyaloclastite, are scarce or absent.

The Mount Cayley volcanic field hosts several good examples of subglacial domes. Ember Ridge (Fig. 4d), consists of six irregular masses of aphanitic to glassy hornblende–phyric andesite. Each mass has a colloform surface, with margins consisting of steeply inclined or vertical cooling units; individual flows are up to 60 m thick, and the summit regions of most outcrops are eroded into irregular knobs and spires. Jointing is fine-scale and complex; columns average 15–25 cm in diameter, although they are commonly significantly smaller (i.e. 5–10 cm) near the top surfaces of some flows.

A more complex series of flows occurs at Slag Hill, near the northern end of the Mount Cayley volcanic field (Fig. 1), the easternmost lobe of which has the characteristics of a subglacial dome. Slag Hill consists of piles of black, glassy, bulbous augite-phyric basaltic andesite flows. Columns have small diameters, variable orientations, and commonly occur as locally radiating masses. The northwestern lobe of Slag Hill is nearly flat-topped, with near-vertical, finely-jointed margins, while the eastern lobe has a more rounded morphology. A small, isolated bluff at the northern end of the Slag Hill pile is flat-topped and steep-sided, and has fine-scale irregular jointing around its margins.

The region around Mount Garibaldi (Fig. 1) also contains numerous dome-like masses of andesite or dacite lava at Mount Brew, the Eenostuck complex, the Sphinx Moraine complex, Round Mountain, Columnar Peak and on the ridge south-east of the Table (Mathews 1958; Green 1977).

The Watts Point volcanic field is a pile of flows at the southernmost end of the GVB (Fig. 1). It comprises 0.02 km^3 of heavily-jointed, sparsely hornblende or pyroxene-phyric dacite lava and breccia (Bye *et al.* 2000). Evidence of quenching is common; columns are 5–40 cm in diameter, with locally radiating patterns, and flows are glassy to fine-grained.

The Monmouth Creek complex (Fig. 1) is a prominent, complex, and enigmatic feature of unknown age west of Squamish. It consists of at least four en echelon dikes which form the ribs of spires rising 60–180 m above a main lava mass (Mathews 1958). The tallest of these spires, the Castle, features continuous horizontal, radiating columnar joints. The spires are mantled by agglutinated breccia near their bases, and jointing extends into the agglutinate. The uppermost flows and spires are dacite (Mathews 1958; Green 1994).

All of the features described above, based on their morphologies, and irregular, commonly vertical cooling surfaces, likely formed by eruption into a confined setting. They cannot be explained by the apparent palaeotopography, and are inferred to have been confined by ice. The Monmouth Creek complex probably represents a series of subglacial domes and dykes, while the other features are subglacial domes.

Vent locations appear to be beneath or near most subglacial domes, based on jointing patterns and the glassiness of some lavas (e.g. Ember Ridge, Fig. 1), and many subglacial domes represent a single extrusive episode. The Ember Ridge deposits likely represent discrete extrusive events which were approximately coeval, based on their similar morphologies, jointing styles, and degrees of erosion (Souther 1980). The Slag Hill deposits are more complex and may represent multiple eruptions in the same location; the western lobe and isolated bluff of Slag Hill have peripheries consistent with eruption against ice, although their top surfaces suggest that eruptions breached the ice surface, and are thus similar to flow-dominated tuyas. The north-eastern lobe of Slag Hill, however, has the characteristics of a subglacial dome.

Characteristics of subglacial domes are (a) fine-scale (<25 cm) columnar jointing; (b) horizontal columns, indicating vertical cooling surfaces; (c) other fine-scale jointing (e.g. flaggy jointing); (d) irregular joint patterns, or joints forming radiating masses, on the top surfaces or sides of flows, indicating locally irregular cooling surfaces; (e) scarcity or lack of primary fragmental material; and (f) edifice shapes and joint patterns that cannot be explained by the apparent palaeotopography. Subglacial domes are interpreted as lava masses that did not breach the ice surface during eruption.

Subglacial flows

Subglacial flows are laterally extensive lava flows with steep, horizontally-jointed margins. The Cheakamus River Valley, on the western margin of the Garibaldi volcanic field (Fig. 1), contains the only known example of this feature. The Cheakamus River Valley has been subjected to episodic eruptions of flat-lying basalt flows. The uppermost flows consist of olivine-plagioclase-phyric basalts with sinuous, anastomosing outcrop patterns, and are commonly described

as 'esker-like' (Mathews 1958). An underlying till is radiocarbon dated at 34 200 ± 800 BP, which correlates with the Olympia Interstade, a non-glacial interval which immediately preceded the Fraser Glaciation (Fulton *et al.* 1976). Columnar jointing is ubiquitous, and is horizontal along the steep sides of the flows and vertical beneath the blocky flow tops. At several locations, pillows or pillow-like features are present in the basal parts of the flows, and some portions of flows are underlain by hyaloclastite breccia.

The Cheakamus Valley lavas appear to have been highly fluid, based on their flow termini, which are commonly less than a metre in thickness. They appear to have been emplaced subglacially, based on the age of the underlying till, the presence of pillows near the bases of some flows, which indicates subaqueous eruption, the horizontal jointing at flow margins, which indicates a vertical cooling surface, and the scale of jointing, which indicates rapid cooling. The source of the Cheakamus Valley flows is unknown (Green *et al.* 1988).

Subglacial flows are characterized by (a) fine-scale jointing; (b) horizontal columns at lateral margins; (c) locally irregular or radial jointing; and (d) outcrops with low aspect ratios, which cover wide areas, and cannot be explained by the apparent palaeotopography. These flows are inferred to have been extruded subglacially, and to have flowed some distance from the vent in tunnels or trenches within the ice sheet (Mathews 1958).

Ice-marginal flows

Ice-marginal flows have subaerial origins, but have steep or vertical, intensely jointed, over-thickened margins, resulting from interaction with ice.

The best-described example of an ice-marginal flow in the GVB is the Barrier (Fig. 4e), located to the NE of Mount Garibaldi, near the Mount Price complex (Fig. 1). An oxidized, rubble-topped, andesite flow stretches from a cone on the western side of Mount Price, Clinker Peak, into the upper reaches of the Rubble Creek Valley. There it terminates in a 200 m cliff, surrounded by debris. A similar cliff occurs in the upper reaches of the Culliton Creek Valley. The current face of the Barrier is a scar from a major landslide during the mid-nineteenth century (Mathews 1952*a*). Other nearby examples of ice-marginal flows of andesite or dacite occur at Paul Ridge, Glacier Pikes and Black Tusk (Green 1977; Green *et al.* 1988).

Pali Dome, in the Mount Cayley volcanic field (Fig. 1) consists of coarsely plagioclase–hypersthene ± hornblende–phyric andesite flows whose apparent source is currently ice-covered (Souther 1980). Proximal parts of flows have large diameter columns (up to 90 cm) overlying scoriaceous, oxidized, flow breccia. Distal portions of flows, however, are finely-jointed; column diameters are commonly less than 20 cm and may be horizontal or in complex radiating masses. Flow termini comprise nearly vertical cliffs which are 100–200 m high, and are locally broken into small spires and knobs (Fig. 4f). The terminal cliffs of the south-eastern flows are flanked by more than 70 m of glassy debris.

Several ice-marginal glaciovolcanic features occur in the Salal Glacier area north of Mount Meager (Fig. 1). This small volcanic field is compositionally distinctive because its lavas are alkaline (Fig. 2). At Logan Ridge, two basanitoid pillowed flows, separated by an 8 m-thick tuff layer, form a steep cliff face (R. B. Lawrence pers. comm., 1979; Lawrence *et al.* 1984). At Ochre Mountain, south-east of Logan Ridge (Fig. 1), there is a thin (<8 m thick) alkali olivine basalt flow with a brecciated (and partially palagonitized) base. The flow shows pervasive but poorly-developed jointing.

Ice-marginal lava flows are inferred to have formed when subaerially-erupted lavas flowed downhill and pooled against ice which occupied lower elevations, based on their joint sizes and orientations, and the lack of palaeotopographic features against which they could have cooled; the Barrier was the first such recognized feature in the GVB (Mathews 1952*a*). Flows such as those at the Barrier and in the Culliton Creek Valley clearly followed the retreat of ice from higher elevations, based on the lack of ice-contact or glacial erosion features at these altitudes. They must, however, have predated the total disappearance of the ice sheet and thus are inferred to have formed during the waning stages of the Fraser Glaciation (Mathews 1952*a*). The tuff layer at Logan Ridge was interpreted as airfall by Lawrence (pers. comm., 1979). However, its thickness, partial palagonitization, relationship to the pillow lavas above and below, and the nearby presence of hyaloclastite suggest that it could be waterlain, suggesting that the Logan Ridge deposit is also an ice-marginal flow.

Ice-marginal flows are useful in delineating the margins of ice sheets. Evidence for ice impoundment of flow fronts includes (a) abundant small-diameter, chaotically-oriented, columnar joints; (b) fine-scale horizontal jointing; and (c) unusually thick and vertically-faced flow termini which cannot be explained by the

apparent palaeotopography. These features are diagnostic, but can easily be lost through erosion because of the inherently unstable nature of ice-impounded flows.

Comparisons with other settings

The best analogues for the glaciovolcanic features found in the GVB derive from the United States Cascades, which has similarities in tectonic setting, lava compositions, topography, and glacial history. Lescinsky & Fink (2000) described many glaciovolcanic features in the Cascades which appear to be similar to those of the GVB.

Tuyas similar to the flow-dominated tuyas of the GVB have not yet been described from other glaciovolcanic regions. This is probably because most descriptions are from regions that are dominated by basaltic edifices (e.g. Jones 1969; Skilling 1994; Smellie & Hole 1997). The only conventional tuyas within the GVB are of basaltic composition (e.g. Tuber Hill; Roddick & Souther 1987). This suggests a correlation between morphology and composition. Most of the non-basaltic glaciovolcanic systems studied have been rhyolites (e.g. Furnes *et al.* 1980, Tuffen *et al.* 2001), and potential analogues to flow-dominated tuyas have not been identified in these systems. Phonolitic glaciovolcanism has been investigated at Hoodoo Mountain volcano in northwestern British Columbia, a steep-sided edifice that, beneath its ice cap, is flat-topped (Edwards & Russell 1994, 1995, 2002; Edwards *et al.* 2002). However, this is a long-lived stratovolcano, which is a poor analogue for the smaller, shorter-lived, monogenetic intermediate centres of the GVB.

The best analogues for the subglacial domes of the GVB are andesitic to rhyolitic domes formed by lava–ice interaction in the United States Cascades, but few studies have focused on their glaciovolcanic attributes (Guffanti & Weaver 1988; Lescinsky & Fink 2000). GVB subglacial domes are unlike the more extensively studied rhyolitic subglacial edifices of Iceland (Furnes *et al.* 1980; Tuffen *et al.* 2001). Icelandic subglacial rhyolitic volcanoes, such as Bláhnúkur, in south-central Iceland, commonly contain lava lobes 5–10 m long set in breccia or hyaloclastite (Furnes *et al.* 1980; Tuffen *et al.* 2001), whereas subglacial domes in the GVB consist of coherent lava masses several hundred metres across, with little or no associated pyroclastic material. At Bláhnúkur, however, there are also several larger (up to 400 m long and 20 m thick) columnar jointed rhyolite flows whose margins indicate cooling against steeply inclined ice walls, and these flows appear to be grossly similar to lava domes and masses found in the GVB (e.g. Ember Ridge).

Features analogous to the Cheakamus River Valley esker-like flows have not yet been identified outside the GVB. Their morphology and outcrop patterns may result from relatively rare events where special conditions for ice thickness, effusion rate, lava properties, and slope, are met. Conversely, the absence of these flow features in the literature may be a reflection of their fragility; the Cheakamus Valley flows are relatively thin, and much of the lava is pervasively jointed, making it easily eroded.

Features indicative of ice-marginal volcanism have been identified in many settings but are notably abundant in the United States Cascades (e.g. Conrey 1991; Lescinsky & Sisson 1998; Lescinsky & Fink 2000) where the relief and topography are similar to that found in the GVB.

Discussion

The differences in morphology and internal characteristics between GVB glaciovolcanic landforms and those described in other regions appear to be primarily a function of composition. Composition controls many important lava properties, including liquidus temperature, viscosity, volatile content, heat capacity, and glass transition temperature. Ultimately, these properties control effusion rates and eruption style and, thus, the forms of many volcanic deposits. In subaqueous settings, for example, viscous siliceous lava flows tend to be thicker and have larger pillows than basaltic flows (Pichler 1965; Furnes *et al.* 1980).

Topography plays a lesser but still significant role in the development of glaciovolcanic deposits in the GVB. Firstly, steep topography enhances erosion rates. Secondly, in an intermittently-glaciated setting such as the GVB, where there are many high-altitude vents, instances of subaerially erupted lavas moving downslope and ponding against ice should be common. This process is recorded, both in the GVB and the Cascades, by numerous exposures of ice-marginal lava flows. Thirdly, topography must influence the ice depth at which eruptions occur. Glaciers should be thickest in the valleys and thinner at high elevations. Eruptions occurring at high elevations, therefore, have less ice available to be melted and are more likely to breach the ice surface. Finally, steep topography will enhance meltwater drainage. The ability

of a subglacial volcano to melt and retain water is an important control on its final lithological characteristics.

Heat transfer considerations

Allen (1980) investigated the heat balance for subglacial basaltic eruptions. He demonstrated that, for average magmatic temperatures and effusion rates, the heat derived from basalt is more than sufficient to melt an ice cavern large enough to accommodate the growing lava pile. However, the heat budgets attending the eruption of mafic and felsic magmas beneath ice can be substantially different (e.g. Hoskuldsson & Sparks 1997).

Heat transfer differences between mafic and felsic magmas arise because of their differences in eruption temperature (*Te*), and the magnitude of the interval between *Te* and the calorimetrically defined glass transition temperature (*Tg*). The value of *Tg* marks the transition from the melt to the glassy state and is defined by marked changes in molar heat capacity, thermal expansivity, and other second order thermodynamic properties; it also corresponds to an increase in viscosity (typically $>10^{13}$ Pa s^{-1}). The calorimetric *Tg* is an important limiting value for magmatic processes because, above *Tg*, rates of nucleation, crystallization, and vesiculation are fast enough to compete with most magmatic and eruptive time scales. Conversely, at temperatures below *Tg*, glass forms, and crystallization and vesiculation may be suppressed. *Tg* is important to heat budgets because crystallization is suppressed below this temperature. This eliminates potential latent heats of crystallization (*L*). Latent heats of vitrification are essentially zero and, thus, the transition from melt to glass does not contribute to the heat budget.

We have calculated the liquidus temperatures and glass transition temperatures for a variety of mafic to intermediate volcanic rock types (Table 3). The basalt compositions are based on glass analyses from Icelandic basalts erupted at the Laki fissure (Thordarson *et al.* 1996) and Herdubreid (Moore & Calk 1991). The intermediate composition analyses are of andesite and dacite samples from the GVB (Fiesinger 1975; Kelman *et al.* 2001). Liquidus temperatures are calculated using MELTS: a model used for the computation of multi-component phase

Table 3. *Compositions of lavas from Garibaldi volcanic belt and Iceland used to compare the differences in liquidus temperatures and glass transition temperatures*

Sample†	KR-1[1]	KR-2[1]	KR-4[1]	KR-10[1]	KR-11[1]	GV31[2]	GV22[2]	gl-1[3]	gl-4[3]	Hr[3]
Rock type†	A	A	A	D	D	D	D	B	B	B
SiO_2	62.18	58.63	62.60	65.99	67.57	64.41	64.81	49.68	49.13	48.70
TiO_2	0.63	0.64	0.62	0.45	0.41	0.52	0.37	2.96	2.00	1.38
Al_2O_3	17.97	18.09	17.93	16.72	16.26	16.38	16.32	13.05	12.03	15.40
Fe_2O_3	4.90	5.83	4.94	4.10	3.68	1.32	1.59	–	–	–
FeO	–	–	–	–	–	2.64	2.20	13.78	13.41	10.70
MnO	0.08	0.10	0.08	0.08	0.08	0.04	0.01	0.22	0.23	0.18
MgO	2.27	4.28	2.25	1.88	1.60	2.46	1.41	5.78	8.47	8.23
CaO	5.73	6.29	5.74	4.27	3.88	5.03	4.37	10.45	11.37	12.80
Na_2O	4.38	4.68	4.37	4.55	4.46	4.92	4.82	2.84	2.47	2.08
K_2O	1.55	1.01	1.56	1.79	1.89	1.63	1.73	0.42	0.39	0.13
P_2O_5	0.27	0.25	0.27	0.18	0.16	0.17	0.20	0.28	0.17	0.16
H_2O^-	0.15	0.26	0.01	0.08	0.22	0.27	1.18	–	–	–
H_2O^+	0.09	0.56	0.11	0.01	0.00	0.07	0.60	–	–	–
Total	100.20	100.63	100.47	100.10	100.21	99.86	99.61	99.46	99.67	99.76
Liquidus (1 atm) and Glass Transition Temperatures (°C) Computed at QFM										
Fe_2O_3‡	0.78	0.92	0.78	0.66	0.59	0.71	0.66	2.33	2.29	1.83
FeO‡	3.71	4.42	3.74	3.1	2.78	3.19	3.04	11.68	11.35	9.05
T_L (anhydrous)	1179	1188	1178	1146	1133	1160	1155	1166	1195	1216
T_L (hydrous)	1162	1135	1170	1140	1118	1136	1047	–	–	–
Tg	1013	1010	1013	1010	1009	1009	1013	900	797	825
T_L–*Tg*	149	125	157	130	109	127	34	266	398	391

*Sample locations: 1, Mount Cayley volcanic field (Kelman *et al.* 2001); 2, Southern Garibaldi Volcanic Belt (Fiesinger 1975); 3, Iceland–Laki (Thordarson *et al.* 1996) and Herdubreid (Moore & Calk 1991).
† A, andesite; D, dacite; B, basalt glass.
‡ Ferric-ferrous contents recalculated at liquidus temperatures for the QFM oxygen buffer.

Table 4. *Physical constants used in calculation of heat budgets attending cooling of basalt and dacite magmas*

	Basalt		Dacite		Ratios dacite/basalt
	Melt	Glass	Melt	Glass	
Te (°C)[1]	1200	–	1125	–	–
Tg (°C)[2]	–	800	–	1000	–
Cp ($J\,mol^{-1}\,K^{-1}$)[3]	50.52	44.00	51.80	44.00	–
L ($J\,mol^{-1}$)[4]	26200	–	29139	–	–
% crystallization	30	–	0	–	–
ΔH–*Tg* ($kJ\,mol^{-1}$)[5]	28.94	–	6.48	–	0.22
ΔH – total ($kJ\,mol^{-1}$)[6]	64.14	–	50.475	–	0.79

1, eruption temperature; 2, glass transition temperature; 3, heat capacity; 4, latent heat of crystallization; 5, heat released from *Te* to *Tg*; 6, heat released from *Te* to 0°C.

equilibria in silicate melts (Ghiorso & Sack 1995). All liquidus calculations were performed at 1 bar pressure, and ferric : ferrous ratios of the melts were fixed by imposing QFM buffered oxygen fugacities (Table 4). Values of T_L were calculated for both anhydrous and hydrous (based on the measured H_2O contents) melt compositions.

We have also calculated the values for the glass transition temperatures of these same melts (Table 4) using the empirical model developed by Russell & Nicholls (1992, 1996). This model predicts the thermodynamic glass transition temperature (*Tg*) as a function of melt composition and is based on a database of over 750 experimental calorimetric heat content measurements on silicate melts and glasses of diverse composition. The model reproduces the experimentally measured values of *Tg* to within 30°C, although it does not account for the effects of H_2O.

Values of *Tg* for basaltic liquids are calculated to vary between 800 and 900°C, implying a T_L–T_g interval of 260 to 400°C. Conversely, the calculated values of *Tg* for the intermediate rocks vary between 1005 and 1015°C, and suggest a much smaller interval between T_L and T_g (105–160°C). Results of the calculations are summarized in Figure 5. Firstly, the calculated values of T_L and *Tg* are compared directly in Figure 5a. Basaltic melts have higher liquidus temperatures and lower values of *Tg* than intermediate compositions. The same data are plotted against the melt composition (SiO_2 content) in Figure 5b. In general, T_L decreases with increasing SiO_2 content, while *Tg* increases with increasing SiO_2. The result is that T_L–T_g decreases markedly as SiO_2 content increases. Melts that have small values of T_L–T_g require only slight cooling to produce glass whilst bypassing crystallization.

Below, we compare semi-quantitatively the energetics of extruding basalt and dacite magmas beneath ice. The heat that could be released by basalt intruding and cooling beneath ice (Fig. 5a) is summarized as:

$$\Delta H_B = \int_{Te}^{Tg} Cp_B\,dT + \int_{Te}^{Tg} L_B\,dT + \int_{Tg}^{Ti} Cp_g\,dT \quad (1)$$

where Cp_B and Cp_g are the average molar heat capacities ($J\,mol^{-1}\,K^{-1}$) of basalt melt and basalt glass, and L_B is the average molar latent heat of crystallization ($J\,mol^{-1}\,K^{-1}$) (cf. Russell *et al.* 1995). The three integral terms in Equation 1 represent the sensible heat (*S*, Fig. 6a) released to the ice by cooling of the basalt from *Te* to *Tg*, the latent heat (*L*, Fig. 6a) liberated by crystallization between *Te* and *Tg*, and the heat released by conductive cooling of the basalt pile from *Tg* to the ambient ice temperature (*Ti*), respectively. Figure 6a shows model results for a basalt erupted at 1200°C and with a *Tg* of 800°C (Table 3). We have allowed for 30% crystallization, assuming that the accelerated cooling rates will inhibit crystallization even in a basaltic system. These calculations suggest a total heat release of just over $60\,kJ\,mol^{-1}$ for a basalt magma.

The heat budget for cooling of dacite beneath ice features several differences. Firstly, dacite will have a lower eruption temperature and could have a different heat capacity (Cp_D). More importantly, the interval separating *Te* and *Tg* for dacite melts is likely to be much smaller than that found in basalts (Fig. 5, Table 4). For example, a typical dacite may have values of *Te* = 1125°C and *Tg* = 1000°C; thus, the dacite *Te*–T_L interval is 125°C v. 400°C for basalts (Fig. 5, Table 4). The implication is that there is substantially less opportunity for crystallization of the dacite and this reduces the total heat

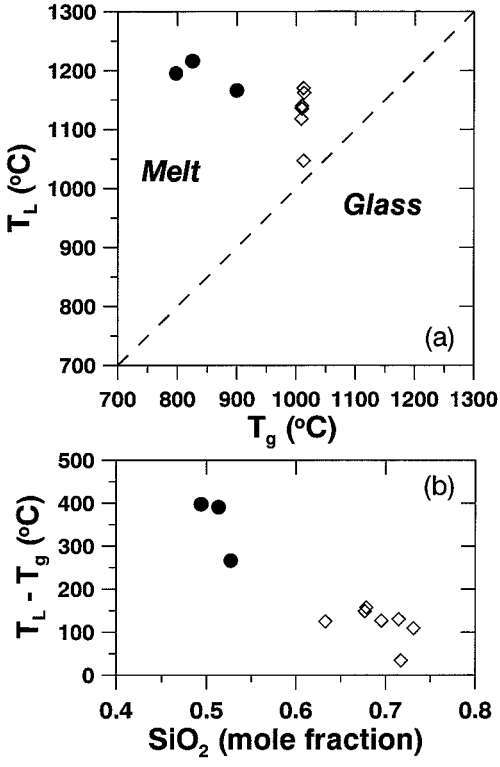

Fig. 5. Comparison of calculated 1-atmosphere liquidus (T_L) and glass transition temperatures (Tg) for melt compositions listed in Table 3. Values of T_L are calculated at 1 bar pressure and at the QFM oxygen buffer using the thermodynamic model MELTS (Ghiorso & Sack 1995). Table 1 reports T_L values for both anhydrous and hydrous compositions; the latter uses the measured H_2O contents of the samples. **(a)** Calculated values of T_L v. Tg for basaltic lavas from Iceland (solid circles) and intermediate lavas from the Garibaldi Volcanic Belt (open diamonds; see Table 4). Dashed line corresponds to equivalence between T_L and Tg where melt would pass through the glass transition temperature. **(b)** Plot showing the difference between T_L and Tg mapped against melt composition (mole fraction SiO_2). In general T_L decreases with increasing SiO_2 content whereas Tg increases with increasing SiO_2 content. The result is that T_L–Tg decreases markedly with increasing SiO_2 content. Melts that have small values of T_L–Tg require only slight cooling to produce glass whilst bypassing crystallization.

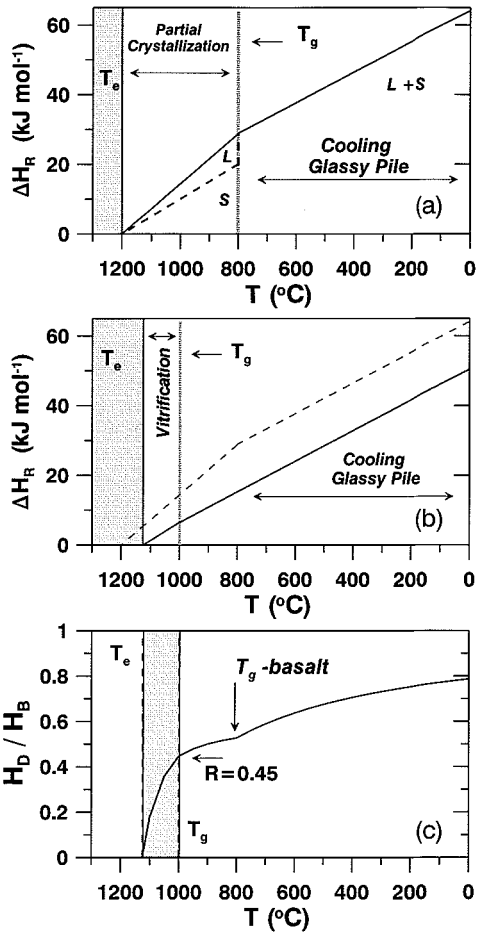

Fig. 6. Model values of heat that would be released by eruption and cooling of lava beneath ice and that could be used to melt ice (see text and Table 4). Thermodynamic calculations are summarized as: **(a)** Heat released (ΔH_R) by a basalt erupted at 1200°C undergoing 30% crystallization before reaching the glass transition temperature ($Tg = 800$°C) and then cooling to ambient ice temperature. Total heat released is a combination of sensible (S) and latent heat of crystallization (L). **(b)** ΔH_R for dacite erupted at 1125°C that reaches its Tg (1000°C) without crystallization and then cools within the ice. Basalt curve (dashed) is shown for reference. **(c)** The ratio of heat released by dacite v. that of basalt plotted against temperature. At the calorimetric Tg, the dacite will have released 45% of the total heat released by the basalt at an equivalent temperature. Over the entire path, dacite releases 70–80% of the total heat released by basalt.

available for melting of the ice. Below, we have modelled the end member system where the accelerated cooling rates prevent crystallization of the dacite by:

$$\Delta H_D = \int_{Te}^{Tg} Cp_D \, dT + \int_{Tg}^{Ti} Cp_g \, dT \qquad (2)$$

The results of this computation are shown in Figure 6b (solid line) and are compared to the heat released by cooling of basalt (dashed line). The dacite releases considerably less heat over its cooling history because the total sensible heat

loss is less (*Te* is lower) and because there is essentially no latent heat of crystallization.

The ratio of ΔH_R for dacite to basalt is shown in Figure 6c. Over the entire cooling interval, dacite magmas release less total heat (80%) than would corresponding volumes of basalt. However, over the interval *Te–Tg*, the heat released by dacite is less than half (45%) of the heat released by basalt over the same temperature interval. Furthermore, at the *Tg* of dacite, the basalt magma is still well above its *Tg*. This is significant because it is the temperature interval above *Tg* that is important to the eruptive process; no crystallization can occur below *Tg*. These calculations point to an important conclusion, that dacite is less able to produce large subglacial caverns; the ice sheet may play a substantially greater role in shaping the volcanic pile than it does in the case of basaltic volcanism.

The scarcity of fragmental deposits

There are apparently few pyroclastic glaciovolcanic deposits (i.e. hyaloclastite) preserved in the GVB, except at basaltic centres. Either such deposits are rare in the GVB, or their scarcity is a result of removal. As such deposits occur in lavas of mafic to felsic compositions elsewhere (e.g. Pichler 1965; Furnes *et al.* 1980; Tuffen *et al.* 2001; Edwards & Russell 2002; Edwards *et al.* 2002), composition cannot be the sole explanation. Below, we discuss the possible factors that may contribute to this apparent scarcity.

Primary fragmentation mechanisms. The formation of primary fragmental volcanic deposits requires the presence of volatile components in the magma or magma–water contact. Kokelaar (1986) divided subaqueous clast-forming processes into four types: (1) explosive release of magmatic volatiles; (2) explosive expansion and collapse of steam formed at magma–water contact surfaces; (3) explosive expansion of steam following enclosure in magma; and (4) cooling-contraction. The first process should depend on the primary volatile content of a magma and its ascent history. The two clast-forming processes related to steam may be potentially controlled by the pressure exerted by overlying ice or water during eruption, or by the amount of direct water–lava contact. The final clast-forming process, cooling-contraction, requires only the presence of water, and may occur at any water depth in a magma of any volatile content.

Primary volatile content and magma ascent history are poorly known for most GVB glaciovolcanic edifices. Green (1977) estimated the water content of Garibaldi Lake region hornblende andesites to be 3.8–4.5 wt% and volatile contents at other GVB volcanoes, although not known, may well be similar. Efficient pre-eruptive degassing would explain a lack of fragmental deposits formed due to primary volatile exsolution. However, there are numerous occurrences of non-glaciovolcanic pyroclastic deposits within the GVB (Mathews 1952*b*, 1958; Read 1977; Souther 1980; Green *et al.* 1988; Stasiuk & Russell 1990; Stasiuk *et al.* 1996; Hickson *et al.* 1999). This suggests that GVB magmas are capable of supporting explosive volcanism. Thus, lack of magmatic volatiles is unlikely to be the reason for the scarcity of intermediate composition fragmental glaciovolcanic deposits in the GVB.

Kokelaar (1986) observed that primary magmatic explosivity and the two steam-related clast-forming processes (magma–water contact surface explosivity and steam entrapment explosivity) are diminished as water depth increases. Thus, great ice thicknesses might inhibit clast formation by these two methods. However, eruptions throughout the GVB have occurred during all phases of glaciation, and eruption must have occurred under ice sheets of a wide range of thicknesses. If ice thickness was the only control on hyaloclastite production, fragmental deposits would form when eruption occurred under thin ice of shrinking glaciers.

If not suppressed by pressure, however, fragmentation related to steam-expansion and cooling-contraction should occur during subglacial eruptions, regardless of a lava's volatile content, unless there is insufficient direct water–lava contact. This would occur if cooling units grew mostly by endogenous intrusion, or if water drained continuously and efficiently from subglacial caverns. Hoskuldsson & Sparks (1997) calculated rates of ice melting in basalt and rhyolite eruptions. They proposed that, if heat exchange efficiency in a basaltic subglacial eruption were greater than approximately 80%, a negative pressure would result for cavities melted into the ice, allowing water to accumulate in the cavity. For less efficient heat exchange, which would be more likely for rhyolitic compositions, cavity pressure would be positive, and water would drain from the cavity. These results suggest that, in, silicic and intermediate subglacial eruptions, less water may be present at vents. This could explain the scarcity of fragmental material in the resultant deposits. Additionally, as discussed above, less heat will be released during eruption of intermediate lavas than in eruption of basaltic lavas, so less water

will be produced through melting, regardless of whether it accumulates or drains. Finally, vents that are perched at high elevations, situated under thin ice and surrounded by steep slopes, are unlikely to support the accumulation of meltwater; the permeable ice and steep topography will combine to keep the ice mass over the vent well-drained (Smellie *et al.* 1993; Smellie & Skilling 1994; Smellie 2000).

GVB subglacial domes lack hyaloclastite, do not form pillows, have steep flow margins featuring fine-scale, chaotically-oriented cooling joints, and commonly have bulbous or colloform surfaces. These features suggest that the lavas have been efficiently impounded by ice but have not necessarily been erupted into standing bodies of water. Outside the GVB, a possible example of eruptive products shaped more by ice than by water occurs at Bláhnúkur, in south-central Iceland, where columnar jointed rhyolite flows show limited evidence for direct lava–water interaction. Calculated potential flow velocities at Bláhnúkur are greater than melting rates would have been by 3–4 orders of magnitude, indicating that ice would have constrained the lava, an hypothesis which is supported by field observations such as joint orientations (Tuffen *et al.* 2001).

Preservation potential. An alternative explanation for the scarcity of fragmental deposits at glaciovolcanic edifices within the GVB may be erosion. Due to high uplift rates and steep, irregular, topography, rates of mass wasting in the GVB are extremely high, and most of the large edifices, such as Mount Cayley, have undergone multiple landslide events (Clague & Souther 1982; Jordan 1987; Evans & Brooks 1991; Lu 1992). The poor consolidation of unwelded fragmental deposits makes them extremely vulnerable to erosion. Additionally, the proportion of supraglacial eruptions, some of which may have been explosive, may be much greater than is suggested by the geologic record, because such deposits are very unlikely to be preserved. Thus, the record of glaciovolcanism in the GVB may not be representative of the original size and number of deposits. However, since fragmental glaciovolcanic deposits do occur at basaltic edifices in the GVB, erosion cannot be the only explanation for their scarcity at intermediate composition edifices.

In summary, the scarcity of fragmental glaciovolcanic deposits in the GVB could potentially be attributed to one or more of the following: suppression of primary magmatic explosivity through insufficient primary volatile content of magmas, pre-eruptive degassing, or high ambient pressure due to thick ice or deep water; suppression of steam-expansion related explosive processes through eruption under thick ice or deep water, or insufficient direct contact between erupting magma and water (due to endogenous growth of cooling units or to efficient draining of water during eruption); suppression of cooling-contraction fragmentation due to insufficient direct contact between magma and water; or, lack of deposit preservation. The factor most likely to be responsible for the scarcity of fragmental glaciovolcanic deposits in the GVB is lack of direct lava–water contact; lack of deposit preservation is probably also influential. Further data on magma volatile contents and effusion rates for the GVB should help to clarify this issue.

Conclusions

Glaciovolcanic processes in the GVB are distinctive, and the products are dominated by landforms different from those of more thoroughly studied regions (e.g. Iceland, the Tuya–Teslin region of northern British Columbia, etc.). Tuyas in the GVB, except those of basaltic composition, are flow-dominated, featuring atypical internal stratigraphy which consists of stacks of finely jointed flows without pillows and with little or no hyaloclastite, and are products of subglacial eruptions which ultimately breached the ice surface. Subglacial domes (rounded, steep-sided, finely jointed lava piles which likely accumulated above or near vents during entirely subglacial eruptions) and ice-marginal features, formed when lava erupted from subaerial vents and pooled against ice downslope, are also common.

The most important control on glaciovolcanic edifice morphology is probably composition, because intermediate lavas, being more viscous and closer to their glass transition temperatures at the time of eruption, release less sensible heat in cooling to the ambient ice temperature, and release less latent heat from crystallization. The efficiency of heat transfer will also influence the accumulation or drainage of meltwater around the vent. Thus, intermediate composition lavas are more likely to pile up as domes directly over vents (as they do subaerially), and edifice morphologies are likely to be strongly influenced by the overriding ice during eruption. The scarcity of fragmental glaciovolcanic deposits at intermediate composition centres in the GVB is probably due to minimization of lava–water interaction during eruption, and to high erosion rates.

Further analysis of glaciovolcanism in the GVB is ongoing and includes: (1) more detailed mapping and sampling of specific glaciovolcanic features for which there are few data; (2) detailed comparative study of the many flow-dominated tuyas and subglacial domes throughout the GVB; (3) quantitative thermodynamic modelling of the interactions between intermediate lava and ice. This ongoing analysis of glaciovolcanism in southwestern British Columbia is also expected to contribute substantially to climate studies by providing additional radiometric dates for glaciovolcanic deposits. These results, when combined with existing databases, will refine our current knowledge of ice distributions in the Canadian Cordillera throughout space and time and will constrain the timing of major glacial events.

This research was supported by the NSERC Research Grants program (R89820 to J. K. Russell) and the Geological Survey of Canada through Project No. 303071 (C. J. Hickson). Funding for the senior author's participation in the Conference on Volcano–Ice Interaction derived, in part, from the Department of Earth & Ocean Sciences at the University of British Columbia. The senior author thanks D. Lui for field assistance, L. Fox for logistical support, and the reviewers J. Moore, J. Stix, and especially J. Smellie. Sampling of volcanic centres in the northern portion of the GVB was made possible through collaboration with N. Green.

References

ALLEN, C. C. 1980. Icelandic subglacial volcanism: thermal and physical studies. *Journal of Geology*, **88**, 108–117.

ARMSTRONG, J. E. 1981. Post-Vashon Wisconsinan glaciation, Fraser Lowland, British Columbia. *Geological Survey of Canada Bulletin*, **322**.

BROOKS, G. R. & FRIELE, P. A. 1992. Bracketing ages for the formation of the Ring Creek lava flow, Mount Garibaldi volcanic field, southwestern British Columbia. *Canadian Journal of Earth Sciences*, **29**, 2425–2428.

BYE, A., EDWARDS, B. R. & HICKSON, C. J. 2000. Preliminary field, petrographic, and geochemical analysis of possible subglacial, dacitic volcanism at the Watts Point volcanic centre, southwestern British Columbia. *Geological Survey of Canada, Current Research*, **2000-A20**.

CLAGUE, J. J. 1980. Late Quaternary geology and geochronology of British Columbia. Part 1: radiocarbon dates. *Geological Survey of Canada Paper*, **80-13**.

CLAGUE, J. J. 1981. Late Quaternary geology and geochronology of British Columbia. Part 2: summary and discussion of radiocarbon-dated Quaternary history. *Geological Survey of Canada Paper*, **80-35**.

CLAGUE, J. J. 1986. The Quaternary stratigraphic record of British Columbia – evidence for episodic sedimentation and erosion controlled by glaciation. *Canadian Journal of Earth Sciences*, **23**, 885–894.

CLAGUE, J. J., HARPER, J. R., HEBDA, R. J. & HOWES, D. E. 1982. Late Quaternary sea levels and crustal movements, coastal British Columbia. *Canadian Journal of Earth Sciences*, **19**, 597–618.

CLAGUE, J. J. & SOUTHER, J. G. 1982. The Dusty Creek landslide on Mount Cayley, British Columbia. *Canadian Journal of Earth Sciences*, **19**, 524–539.

CLAGUE, J. J., EVANS, S. G., RAMPTON, V. N. & WOODSWORTH, G. J. 1995. Improved age estimates for the White River and Bridge River tephras, western Canada. *Canadian Journal of Earth Sciences*, **32**, 1172–1179.

CONREY, R. M. 1991. *Geology and petrology of the Mt. Jefferson area, High Cascade Range, Oregon*. PhD thesis, Washington State University.

DENTON, G. H. & STUIVER, M. 1967. Late Pleistocene glacial stratigraphy and chronology, northeastern St. Elias Mountains, Yukon Territory, Canada. *Geological Society of America Bulletin*, **78**, 485–510.

EDWARDS, B. R. & RUSSELL, J. K. 1994. Preliminary stratigraphy of Hoodoo Mountain volcanic centre, northwestern British Columbia. *Cordilleran and Pacific margin*. Geological Survey of Canada, Current Research, **1994-A**, 69–76.

EDWARDS, B. R. & RUSSELL, J. K. 1995. Revised stratigraphy for the Hoodoo Mountain volcanic centre, northwestern British Columbia. *Cordilleran and Pacific margin*. Geological Survey of Canada, Current Research, **1995-A**, 105–115.

EDWARDS, B. R. & RUSSELL, J. K. 2002. Glacial influences on morphology and eruptive products of Hoodoo Mountain volcano, Canada. *In*: SMELLIE, J. L. & CHAPMAN, M. G. (eds) *Volcano–Ice Interaction on Earth and Mars*. Geological Society, London, Special Publications, **202**, 179–194.

EDWARDS, B. R., RUSSELL, J. K. & ANDERSON, R. G. 2002. Subglacial, phonolitic volcanism at Hoodoo Mountain volcano, northern Canadian Cordillera. *Bulletin of Volcanology*, **64**, 254–272.

EVANS, S. G. & BROOKS, G. R. 1991. Prehistoric debris avalanches from Mount Cayley volcano, British Columbia. *Canadian Journal of Earth Sciences*, **28**, 1365–1374.

FIESINGER, D. W. 1975. *Petrology of the Quaternary volcanic centres in the Quesnel Highlands and Garibaldi Provincial Park areas, British Columbia*. PhD thesis, University of Calgary.

FULTON, R. J. 1971. Radiocarbon geochronology of southern British Columbia. *Geological Survey of Canada Paper*, **71-37**.

FULTON, R. J. 1984. Quaternary glaciation, Canadian Cordillera. *In*: FULTON, R. J. (ed.) *Quaternary Stratigraphy of Canada: a Canadian Contribution to IGCP Project 24*. Geological Survey of Canada Paper, **84-10**, 39–48.

FULTON, R. J., ARMSTRONG, J. E., FYLES, J. G. & EASTERBROOK, D. J. 1976. Stratigraphy and palynology of late Quaternary sediments in the Puget Lowland, Washington. *Geological Society of America Bulletin*, **87**, 153–156.

FURNES, H., FRIDLEIFSSON, I. B. & ATKINS, F. B. 1980. Subglacial volcanics – on the formation of acid hyaloclastites. *Journal of Volcanology and Geothermal Research*, **8**, 95–110.

GHIORSO, M. S. & SACK, R. O. 1995. Chemical mass transfer in magmatic processes; IV, A revised and internally consistent thermodynamic model for the interpolation and extrapolation of liquid-solid equilibria in magmatic systems at elevated temperatures and pressures. *Contributions to Mineralogy and Petrology*, **119**, 197–212.

GREEN, N. L. 1977. *Multistage Andesite Genesis in the Garibaldi Lake Area, Southwestern British Columbia.* PhD thesis, University of British Columbia.

GREEN, N. L. 1994. Mechanism for middle to upper crustal contamination: evidence from continental-margin magmas. *Geology*, **22**, 231–234.

GREEN, N. L., ARMSTRONG, R. L., HARAKAL, J. E., SOUTHER, J. G. & READ, P. B. 1988. Eruptive history and K–Ar geochronology of the late Cenozoic Garibaldi volcanic belt, southwestern British Columbia. *Geological Society of America Bulletin*, **100**, 563–579.

GRIBBIN, J. R. 1990. *Hothouse Earth.* Grove Weidenfeld, New York.

GUFFANTI, M. & WEAVER, C. S. 1988. Distribution of late Cenozoic volcanic events in the Cascade Range: Volcanic arc segmentation and regional tectonic considerations. *Journal of Geophysical Research*, **93**, 6513–6529.

HICKSON, C. J. 1987. *Late Cenozoic rocks of the Wells Gray – Clearwater area, British Columbia.* PhD thesis, University of British Columbia.

HICKSON, C. J. 1994. Character of volcanism, volcanic hazards, and risk, northern end of the Cascade magmatic arc, British Columbia and Washington state. *In*: MONGER, J. W. H. (ed.) *Geology and Geologic Hazards of the Vancouver Region, Southwestern British Columbia.* Geological Survey of Canada Bulletin, **481**, 231–250.

HICKSON, C. J., MOORE, J. G., CALK, L. & METCALFE, P. 1995. Intraglacial volcanism in the Wells Gray – Clearwater volcanic field, east-central British Columbia, Canada. *Canadian Journal of Earth Sciences*, **32**, 838–851.

HICKSON, C. J., RUSSELL, J. K. & STASIUK, M. V. 1999. Volcanology of the 2350 B.P. eruption of Mount Meager Volcanic Complex, British Columbia, Canada: implications for hazards from eruptions in topographically complex terrain. *Bulletin of Volcanology*, **60**, 489–507.

HOSKULDSSON, A. & SPARKS, R. S. J. 1997. Thermodynamics and fluid dynamics of effusive subglacial eruptions. *Bulletin of Volcanology*, **59**, 219–230.

IRVINE, T. N. & BARAGAR, W. R. A. 1971. A guide to the chemical classification of the common volcanic rocks. *Canadian Journal of Earth Sciences*, **8**, 523–548.

JONES, J. G. 1966. Intraglacial volcanoes of southwest Iceland and their significance in the interpretation of the form of the marine basaltic volcanoes. *Nature*, **212**, 586–588.

JONES, J. G. 1969. Intraglacial volcanoes of the Laugarvatn region, southwest Iceland, I. *Quarterly Journal of the Geological Society, London*, **124**, 197–211.

JONES, J. G. 1970. Intraglacial volcanoes of the Laugarvatn region, southwest Iceland, II. *Journal of Geology*, **78**, 127–140.

JORDAN, P. 1987. Impacts of mass movement events on rivers in the southern Coast Mountains, British Columbia: a summary report. *Environment Canada Water Resources Branch*, **IWD-HQ-WRB-55-87-3**.

KELMAN, M. C., RUSSELL, J. K. & HICKSON, C. J. 2001. Preliminary petrography and chemistry of Quaternary volcanoes of the Mount Cayley volcanic field, British Columbia. *Geological Survey of Canada, Current Research*, **2001-A.**

KLASSEN, R. W. 1978. A unique stratigraphic record of late Tertiary–Quaternary events in southeastern Yukon. *Canadian Journal of Earth Sciences*, **15**, 1884–1886.

KOKELAAR, P. 1986. Magma–water interactions in subaqueous and emergent basaltic volcanism. *Bulletin of Volcanology*, **48**, 275–289.

LAWRENCE, R. B., ARMSTRONG, R. L. & BERMAN, R. G. 1984. Garibaldi Group volcanic rocks of the Salal Creek area, southwestern British Columbia: alkaline lavas on the fringe of the predominantly calc-alkaline Garibaldi (Cascade) volcanic arc. *Journal of Volcanology and Geothermal Research*, **21**, 255–276.

LEBAS, M. J., LE MAITRE, R. W., STRECKEISEN, A. & ZANETTI, B. 1986. Chemical classification of volcanic rocks. *Journal of Petrology*, **68**, 277–279.

LEONARD, E. M. 1995. A varve-based calibration of the Bridge River tephra fall. *Canadian Journal of Earth Sciences*, **32**, 2098–2102.

LESCINSKY, D. T. & FINK, J. H. 2000. Lava and ice interaction at stratovolcanoes: Use of characteristic features to determine past glacial extents and future volcanic hazards. *Journal of Geophysical Research*, **105**, 23 711–23 726.

LESCINSKY, D. T. & SISSON, T. W. 1998. Ridge-forming, ice-bounded lava flows at Mount Rainier, Washington. *Geology*, **26**, 351–354.

LU, Z. Y. 1992. Prehistoric debris avalanches from Mount Cayley volcano, British Columbia: Discussion. *Canadian Journal of Earth Sciences*, **29**, 1342–1343.

MATHEWS, W. H. 1947. 'Tuyas', flat-topped volcanoes in northern British Columbia. *American Journal of Science*, **245**, 560–570.

MATHEWS, W. H. 1951. The Table, a flat-topped volcano in southern British Columbia. *American Journal of Science*, **249**, 830–841.

MATHEWS, W. H. 1952*a*. Ice-dammed lavas from Clinker Mountain, southwestern British Columbia. *American Journal of Science*, **250**, 553–565.

MATHEWS, W. H. 1952*b*. Mount Garibaldi, a supraglacial Pleistocene volcano in southwestern British Columbia. *American Journal of Science*, **250**, 81–103.

MATHEWS, W. H. 1957. Petrology of Quaternary volcanics of the Mount Garibaldi map-area,

southwestern British Columbia. *American Journal of Science*, **255**, 400–415.

MATHEWS, W. H. 1958. Geology of the Mount Garibaldi map-area, southwestern British Columbia, Canada. Part II. Geomorphology and Quaternary volcanic rocks. *Bulletin of the Geological Society of America*, **69**, 161–178.

MOORE, J. G. & CALK, L. C. 1991. Degassing and differentiation in subglacial volcanoes, Iceland. *Journal of Volcanology and Geothermal Research*, **46**, 157–180.

PICHLER, H. 1965. Acid hyaloclastites. *Bulletin of Volcanology*, **28**, 293–310.

READ, P. B. 1977. Meager Creek volcanic complex, southwestern British Columbia. *Geological Survey of Canada Paper*, **77-1A**, 277–281.

READ, P. B. 1990. Mount Meager Complex, Garibaldi Belt, southwestern British Columbia. *Geoscience Canada*, **17**, 167–174.

RODDICK, J. C. & SOUTHER, J. G. 1987. Geochronology of Neogene volcanic rocks in the northern Garibaldi Belt, British Columbia. Radiogenic Age and Isotope Studies, Report 1. *Geological Survey of Canada Paper*, **87-2**, 21–24.

ROHR, K. M. M., GOVERS, R. & FURLONG, K. P. 1996. A new plate boundary model for the Pacific-North American-Juan de Fuca triple junction, Slave-Northern Cordillera Lithospheric Evolution (SNORCLE) and Cordilleran Tectonics Workshop. *In*: *Lithoprobe Report 50: British Columbia, Canada.* Lithoprobe Secretariat for the Canadian Lithoprobe Program, 213–214.

RUSSELL, J. K., EDWARDS, B. R. & SNYDER, L. D. 1995. Volatile production possibilities during magmatic assimilation: Heat and mass-balance constraints. *In*: J. F. H. Thompson (ed.) *Short Course on Magmas, Fluids, and Ore Deposits.* Mineralogical Association of Canada, 1–24.

RUSSELL, J. K. & NICHOLLS, J. 1992. The glass transition temperature in natural systems: Empirical calibration and application. *EOS*, **73**, 600.

RUSSELL, J. K. & NICHOLLS, J. 1996. Petrological perspectives on the calorimetrically-defined glass transition temperature (Tg). *The Physics of Explosive Volcanic Eruptions, Arthur Holmes European Research Conference, Santorini, Program with Abstracts*, **2**.

SHACKLETON, N. J. & OPDYKE, N. D. 1973. Oxygen-isotope and palaeomagnetic stratigraphy of equatorial Pacific core V28–238: oxygen isotope temperatures and ice volumes on a 10^5 year and 10^6 year scale. *Quaternary Research*, **3**, 39–55.

SHERROD, D. R. & SMITH, J. G. 1990. Quaternary extrusion rates of the Cascade Range, northwestern United States and southern British Columbia. *Journal of Geophysical Research*, **95**, 19474–19645.

SKILLING, I. P. 1994. Evolution of an englacial volcano: Brown Bluff, Antarctica. *Bulletin of Volcanology*, **56**, 573–591.

SMELLIE, J. L. 2000. Subglacial eruptions. *In*: SIGURDSSON, H. (ed.) *Encyclopedia of Volcanoes.* Academic Press, San Diego, 403–418.

SMELLIE, J. L. & Hole, M. J. 1997. Products and processes in Pliocene–Recent, subaqueous to emergent volcanism in the Antarctic Peninsula: examples of englacial Surtseyan volcano construction. *Bulletin of Volcanology*, **58**, 628–646.

SMELLIE, J. L., HOLE, M. J. & NELL, P. A. R. 1993. Late Miocene valley-confined subglacial volcanism in northern Alexander Island, Anarctic Peninsula. *Bulletin of Volcanology*, **55**, 273–288.

SMELLIE, J. L. & SKILLING, I. P. 1994. Products of subglacial volcanic eruptions under different ice thicknesses: two examples from Antarctica. *Sedimentary Geology*, **91**, 115–129.

SOUTHER, J. G. 1980. Geothermal reconnaissance in the central Garibaldi Belt, British Columbia. *Geological Survey of Canada, Current Research, Part A*, **80-1A**, 1–11.

SOUTHER, J. G. 1992. Volcanic regimes. *In*: GABRIELSE, H. & YORATH, C. J. (eds) *Geology of the Cordilleran Orogen in Canada.* Geological Survey of Canada, Ottawa, 459–490.

SOUTHER, J. G. & YORATH, C. J. 1991. Neogene Assemblages *In:* GABRIELSE, H. & YORATH, C. J. (eds) *Geology of the Cordilleran Orogen in Canada.* Geological Survey of Canada, Ottawa, 373–401.

STASIUK, M. V. & RUSSELL, J. K. 1990. The Bridge River assemblage in the Meager Mountain volcanic complex, southwestern British Columbia. *Geological Survey of Canada, Current Research, Part E*, **90-1E**, 227–233.

STASIUK, M. V., RUSSELL, J. K. & HICKSON, C. J. 1996. Distribution, nature, and origins of the 2400 BP eruption products of Mount Meager, British Columbia: Linkages between magma chemistry and eruption behaviour. *Geological Survey of Canada Bulletin*, **486**, 1–27.

THORDARSON, T., SELF, S., ÓSKARSSON, N. & HULSEBOSCH, T. 1996. Sulfur, chlorine, and fluorine degassing and atmospheric loading by the 1783–1784 AD Laki (Skaftár Fires) eruption in Iceland. *Bulletin of Volcanology*, **58**, 205–225.

TUFFEN, H., GILBERT, J. & MCGARVIE, D. 2001. Products of an effusive subglacial rhyolite eruption: Bláhnúkur, Torfajökull, Iceland. *Bulletin of Volcanology*, **63**, 179–190.